ELSEVIER

Biophysical Chemistry 53 (1994) 5–14

Biophysical Chemistry

Image plate detectors for macromolecular neutron diffractometry

F. Cipriani [a,*], F. Dauvergne [a], A. Gabriel [a], C. Wilkinson [a], M.S. Lehmann [b]

[a] *EMBL Outstation, Avenue des Martyrs, F38042 Grenoble, France*

[b] *ILL, Avenue des Martyrs, F38042 Grenoble, France*

Received 28 October 1993; revised 18 January 1994; accepted 30 January 1994

Abstract

Neutron diffraction studies of macromolecules require large position sensitive detectors. It is proposed that such a device can be based on image plate technology, which relies on re-usable photostimuable phosphors, combined with a neutron to γ-ray converter. Design parameters such as the best wavelength for the neutron radiation and the optimum sample to detector distance are discussed, and a design for a cylindrical detector is outlined. Presently a prototype of such a detector is being built, and the very first test-recording of an X-ray diffraction pattern from a protein crystal is presented.

Keywords: Protein crystallography; Neutron position-sensitive detection; Image plate

1. Introduction

In recent years there has been an explosive increase in the amount of three-dimensional structural information available for molecular biology. Most of this has come from X-ray diffraction studies of protein or nucleic acid crystals giving the atomic positions of the structurally ordered atoms in the crystals. However, only the non-hydrogen atom positions are normally obtained in this way, while the hydrogen atoms, which have a very low scattering power for X-rays, must be found by different methods.

In total the hydrogen atoms constitute between a third and half of the atoms in a macromolecule, and the position of a fair number of these, for example many of the aliphatically bound hydrogen atoms, can be predicted when the location of the involved carbon atoms are known. For the more labile hydrogen atoms such as those involved in acidity, or the hydrogen atoms bound in the water molecules, the situation is different, and these normally have to be located by a diffraction measurement.

As the scattering length of hydrogen for neutrons is comparable to that of the other atoms, neutron diffraction offers an attractive means to study hydrogen atoms in macromolecules [1]. Moreover, there is a large difference between the scattering lengths of hydrogen ($b_H = -3.7$ fm) and deuterium ($b_D = 6.6$ fm) and this allows different aspects of the crystallized biological system to be outlined and accentuated by selective deuteration [2]. In this case the studies are typically done at low resolution, and the goal is to identify the content of different parts of the macromolecule or its environment, most often when these are not sufficiently ordered to be studied by high-resolution X-ray diffraction.

In most cases a neutron diffraction study therefore acts as a follow-up to the X-ray diffraction analysis, and is complementary to it. It is normally not aimed at solving the structure, but assumes that this has been

* Corresponding author.

SSDI 0301-4622(94)00071-Q

done. Its main goal is to deal with the questions that, for the reasons just given, cannot be answered from the X-ray data.

Unfortunately however, the relatively low intensity of neutron sources sets limits to its applicability. Millimeter size crystals are required, but can only be obtained in a small number of cases. Considerable effort has therefore gone into the enhancement of the diffractometer performance. This can be achieved by the use of large position sensitive detectors, and several diffractometers are now equipped with those [3–7]. Likewise, suggestions have been made to increase the wavelength band on steady state reactors [8] and to employ the large wavelength range of spallation sources [3].

Traditionally, position sensitive detectors for neutrons have been gas-filled wire detectors based on the high neutron capture of ^{3}He or ^{10}B. They are real-time devices with a high detection efficiency and a resolution which at best is around 1 mm. Another possibility is films, where the neutrons are converted into electromagnetic radiation recorded on a photographic film [9], and this approach has been used for many years both in topography [10] and in Laue diffraction [11] employing a number of different converters combined with X-ray films. Most recently the use of the storage phosphors, the 'image-plates' routinely employed in X-ray experiments [12], has been proposed and tested for neutron detection [13,14].

Although image-plates have the drawback of being accumulating detectors with a time consuming reading procedure, the detection surface can be made very large and there is a wide range of freedom in the choice of detector shape. A prototype image-plate detector for neutron measurements is therefore presently being constructed and is reported on here.

2. Image plates for neutrons

Image plates are flexible sheets about 500 μm thick, which have been coated with an approximately 150 μm layer of finely powdered photostimuable phosphor combined with an organic binder. The photostimuable material is most commonly BaFBr doped with Eu^{2+} ions and when irradiated with X-rays or γ-rays electrons liberated by ionising Eu^{2+} to Eu^{3+} are trapped in states just below the conduction band, which has been created by the substitution of Eu for Ba.

The decay time of the electrons in this trapped state is many hours, and the radiation falling on the plate over an extended time can thus be stored for final readout. This is done by photostimulation with visible radiation, normally with the use of a He–Ne laser. The emitted blue light is measured with a photomultiplier, and by scanning the plate the radiation can be recorded as a function of position. The photostimulation also serves to erase the plate, but this can furthermore be done by exposing the plate to an intense source of visible light.

To make the image plates sensitive to neutrons a neutron to X-ray/γ-ray converter is required. A good candidate is gadolinium, which has a very strong (n,γ) resonance to thermal neutrons [15,16] producing both a wide range of kilo-electron volt γ-rays, many of which can be detected by the image plate, and a cascade of conversion electrons which can also stimulate the phosphor.

In practical terms the conversion process can be done in two ways, namely either by placing a thin plate in front of the X-ray image plate or by adding a gadolinium compound to the plate.

In the first case gadolinium is either present as a thin plate of metal or as a thin plate of aluminium covered with Gd_2O_3 paint. The main source of image plate activation is the γ-rays, as the path length in gadolinium for the conversion electrons is very short. Indeed, as gadolinium is a heavy metal it also absorbs the γ-rays, and there is an optimal thickness balancing the neutron and the γ-ray absorption in the material. The neutron cross-section varies with wavelength, so the optimal thickness will also vary. Because of the complex distribution of γ-rays this is nearly impossible to estimate theoretically, but a simple model assuming 1.1 Å neutrons and 8 keV output γ-rays [14] gives an optimum of 7 μm gadolinium and 34% efficiency for absorption. The neutron absorption increases with wavelength, and at 4 Å the efficiency is as high as 81%.

The limitation in absorption efficiency is the main factor restraining the detective quantum efficiency (DQE), which is near 100% for the X-ray case [12]. The DQE is defined as the ratio of the squares of the signal to noise ratios of the input and output signals. This was measured for the Gd containing plate at a wavelength of 2.2 Å. The input signal to noise ratio

was obtained by measuring the mean neutron flux and its variance, while the output signal-to-noise ratio was determined by sampling over a number of smaller areas which are parts of a large homogeneously neutron irradiated zone. The value found was $25 \pm 5\%$, in agreement with the value of 18% determined at a wavelength of 1.8 Å by von Seggern et al. [17].

The main advantage at present of a combined converter/image plate system is that X-ray sensitive plates are commercially available. There are however a number of drawbacks in using a composite system. One is that the converter plate has to be removed before reading, which might be cumbersome for an on-line reading system. Another is that the resolution is reduced compared to the plates containing gadolinium. Unfortunately gadolinium containing plates are not generally available. Some specimens were however fabricated by Siemens, Erlangen, and one of these was made available to us for test. They contain 20% by weight of Gd_2O_3.

Fig. 1 shows a comparative test of the two types of plates. Both kinds obviously give a resolution which would be sufficient for the study of diffraction from millimeter large crystals, but the plate holding gadolinium as a component has the best resolution and a lower background. These differences can be explained by the differences in the photo stimulation process. This can be obtained either by γ-rays which are long range or by electrons which are short range. For the case where the converter is separated from the image plate the activation of the phosphor is entirely by γ-rays while the electron cascade also produced in the (n,γ) resonance process ends up as additional γ-rays of all energies emitted from the Gd converter. These will all have different path lengths through the phosphor thus giving less sharp response and higher background. When gadolinium is embedded in the image plate the cascade of electrons can directly stimulate the phosphor at short range and the total γ-ray production will be reduced, leading in unison to higher resolution and less background.

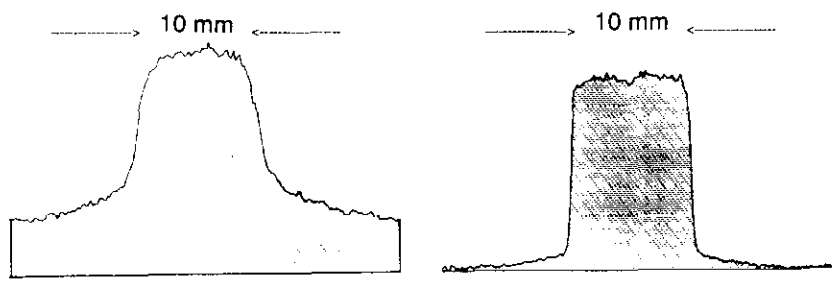

Fig. 1. Two sections through recordings of a neutrons beam. The size of the beam was 1 cm, and the flux was the same for the two measurements. To the left is a beam recorded with a gadolinium plate placed in front of the X-ray image plate. The graph to the right is obtained with the gadolinium containing plate fabricated by Siemens [13].

It is possible to get an estimate of the spatial resolution by fitting the data for the Gd containing image plate to the edge-response function [18]

$$\Gamma(x) = k_1 + k_2 \arctan[\,\lambda(x - x_o)\,],$$

where $\Gamma(x)$ is the number of counts as a function of the position x on the plate, k_1 and k_2 are related to the scalefactor, the absorption coefficient and the thickness of the plate that defines the edge, x_o is the edge position and λ the resolution parameter. By a least-squares fit a value of λ of 18 ± 1 cm^{-1} was found for the case with converter outside the image plate, while the value was 90 ± 5 cm^{-1} with Gd embedded in the plate. Similar differences have been observed by von Seggern et al. [17].

3. A possible experimental geometry

A steady state reactor source offers a wide spectrum of wavelengths giving good flux in the range from about 0.7 Å to about 2 Å from a thermal source, e.g. the reactor core, and from about 3 Å to about 7 Å at the exit of a typical neutron guide, located at a cold source. The wavelength can thus be tuned for optimal data recording. For large unit cells the number of reflections active at any orientation is very large and the angle between the individual reflections small. To overcome the problem of overlap between neighbouring reflections it is therefore useful to increase the wavelength and eventually to move the detector far away from the sample.

For macromolecular studies the maximum wavelength is eventually defined by the minimum d spacing that can be reached. This will normally lie between 1.5 and 2.0 Å, so the maximum wavelength λ should be between 3 and 4 Å, and is thus suitable placed within the available cold source spectrum. Moreover, it is worth noting that an increase in wavelength can increase the recorded number of counts on the detector. If we consider using a quasi-Laue geometry as proposed for an instrument at a steady state reactor [8],

then the total intensity for a Laue spot with indices *hkl* will be

$$I(hkl) = \phi(\lambda)V_s[\,F(hkl)/V_c]^2(\lambda^4/2\sin^2\Theta) \text{ neutrons/s}$$
$$= 2\phi(\lambda)V_s[\,F(hkl)\lambda d_{hkl}/V_c]^2 \text{ neutrons/s},$$

where $F(hkl)$ is the structure amplitude of the reflection with d spacing d_{hkl} and Bragg reflection angle 2Θ, $\phi(\lambda)$ is the differential neutron flux at the sample and V_s and V_c are the sample and unit cell volumes, respectively. The observed intensity is therefore proportional to λ^2, and there is everything to gain by increasing the wavelength. It should however be stressed that the proportionality factors involved are sensitive to the background if we require measurements to a given precision, and we shall discuss this in more detail.

Hydrogen has a very high cross-section for incoherent scattering, and this will for all hydrogen containing compounds be the essential contribution to the background. The background is then given by

$$B_{\text{kinc}} = \phi(\lambda)\Delta\lambda[\,V_s/V_c][\,\textstyle\sum\sigma_{\text{inc}}(\lambda)/4\pi] \times \text{neutrons/s/sterad}, \quad (2)$$

where $\Delta\lambda$ is the wavelength range and $\Sigma\sigma_{\text{inc}}(\lambda)$ is the total incoherent background cross-section of the atoms in one unit cell, coming mainly from the hydrogen atoms. It has been found that the incoherent scattering cross section of hydrogen increases with the wavelength from about 35 barns at 0.8 Å [19] to about 85 barns at 5 Å [20], at least in water.

The image plate is a cumulative counter, so the arrival of neutrons is governed by Poisson statistics. The creation of colour centers and the readout is ruled by a number of processes which are either Poisson or binomial of nature [12]. For both of these types of processes the variance is proportional to the mean. For Poisson statistics the proportionality factor is unity, while for the binomial process the mean (of a successful outcome) is multiplied by the probability for failure in order to get the variance. The read-off efficiency can be made very high [12], so in the binomial processes the probability of failure is low, and the proportionality factor is therefore small. Consequently we can expect the dominating term to be Poisson statistical, and we shall thus assume that $\text{var}(I) = \sigma^2(I) = I$. Likewise, for the generalized argument we will set the detector efficiency to 100%.

A Bragg reflection with intensity $I(hkl)$ neutrons/sec. covering p detector elements is now measured for t sec and at the same time the background is estimated from q elements outside the peak with β neutrons/element/s. The intensity recorded for the Bragg peak is $[I(hkl)+B]t$, where the background under the peak is B neutrons/s., i.e. $B = p\beta t$. The intensity is then

$$I(hkl)t = [\,I(hkl)+B]t - (p/b)b\beta t,$$

and the variance will be

$$\sigma^2(I(hkl)t) = [\,I(hkl)+B]t + (p/b)^2 b\beta t,$$

which can be rewritten as

$$\sigma^2(I(hkl)t) = [\,I(hkl)+B(1+p/b)\,]t.$$

The relative precision is then

$$\frac{\sigma(I(hkl)t)}{I(hkl)t} = \frac{\sqrt{1+\dfrac{B}{I(hkl)}\left(1+\dfrac{p}{q}\right)}}{\sqrt{I(hkl)t}}.$$

For experiments with large unit cells and incoherent scattering the signal will be lower than the background, and therefore

$$\frac{\sigma(I(hkl)t)}{I(hkl)t} \approx \frac{\sqrt{\dfrac{B}{I(hkl)}\left(1+\dfrac{p}{q}\right)}}{\sqrt{I(hkl)t}}.$$

The time to reach an experimental precision of f for $\sigma(I(hkl)t)/I(hkl)t$ is then

$$t \approx \left(1+\frac{p}{q}\right)\frac{B}{I(hkl)^2 f^2}$$

and for a typical experiment with $p \approx q$ this gives

$$t \approx \frac{2B}{I(hkl)^2 f^2}. \quad (3)$$

The background under a Bragg peak will of course be determined by the spot size. For a beam coming from a neutron guide the divergence is proportional to λ, and consequently the area of the spot is proportional to λ^2. Combining this with (1), (2) and (3), and neglecting terms that do not depend on λ, the measurement time will then have the proportionality

$t \approx \sum \sigma_{inc}(\lambda) / \phi(\lambda) \lambda^2$.

There is thus still a favorable λ dependence for the measurement time, but it is in this simple approximation also directly affected by the amount of incoherent scattering from the specimen. A reduction of the incoherent scattering by partial or complete deuteration of the protein is therefore of great importance.

Under some conditions the effect of the background can be reduced by moving the detector further away from the sample. The incoherent scattering will be spread over a larger area, and there will thus be less counts under the Bragg peak, assuming that its size does not grow in the same proportion. The requirement for this is that the size of the spot on the detector is governed by the crystal dimension rather than by the divergence of the beam. Otherwise nothing is gained by moving the detector further away. The optimal choice of distance is therefore reached at the point where the effect of divergence becomes dominant.

In the present case the beam divergence from a Ni-coated neutron guide is 0.0031 λ rad full width at half height (λ in Å), and the spot size will therefore be approximately $2 \times 0.0031\ \lambda L$, where L is the distance from the sample to the detector. The optimum will be given by the condition

$$2 \times 0.0031\ \lambda L > D, \qquad (4)$$

where D is the dimension of the crystal. Assuming this to be at maximum 2 mm we find $L > 100$ mm for a wavelength of 3 Å.

The requirement for the detector is therefore that it must cover angles to high 2Θ in order to reach the smallest d spacing and it should be more than 10 cm away from the sample. Moreover, the resolution should be sufficient to record the Bragg spot in some detail, and should thus be well below 1 mm.

4. A cylindrical detector

The ideal detector should therefore be a spherical shaped device with a radius of more than 10 cm. Using an image plate type detector the read-off would be quite difficult, and the next best to a sphere, a cylinder, was therefore chosen, leading to the geometry of the classical oscillation camera [21].

Fig. 2 shows the first design of such a detector, outlining the general idea. From the above considerations the diameter was chosen to be slightly larger than the minimum, namely 30 cm, while the length of the cylinder was chosen to be 40 cm. The crystal is placed at the center of this cylinder, and to exhaust reciprocal space rotated around the cylinder axis. With the parameters chosen, the blind zone near the rotation axis is a cone with an opening angle of less than 45°, so if necessary the full reciprocal space can be recorded for two orientations of the crystal.

The crystal rotation axis is planned vertical with a large diameter aperture at the top for easy access, and the axis holding the crystal goniometer coming from below. The beam enters the detector surface through a small hole and can continue through another hole on the other side into a remote beam-stop.

Measurements will be done in step scanning mode where the step is determined by $\Delta\lambda$. For monochromatic radiation it is probably around 0.1°, while of course for quasi-Laue techniques it will be much larger. The diffracted neutrons go though the thin aluminium cylinder and though the storage phosphor located on the outer side of the cylinder. When the recording is complete, and the cylinder is read off in a phonographic mode with the reading head moving slowly vertically

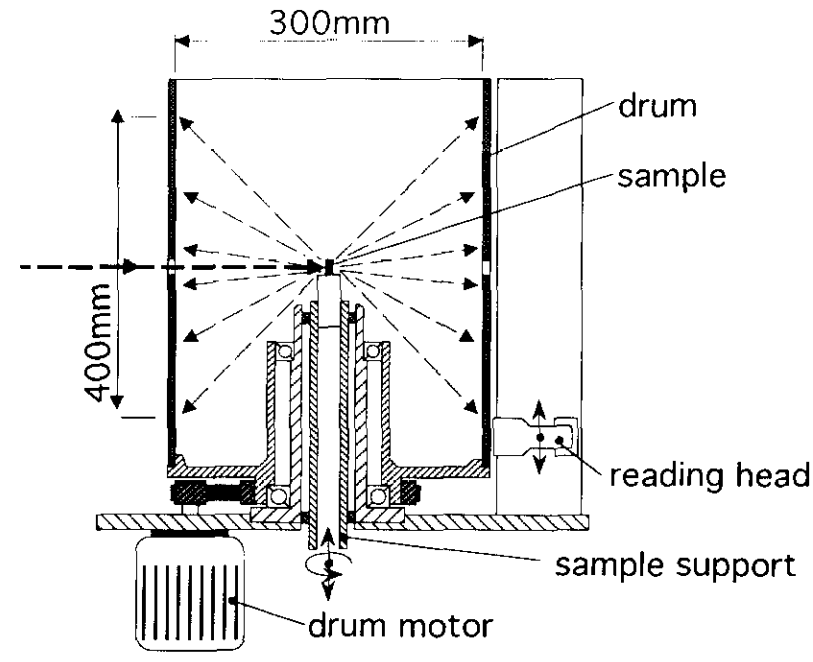

Fig. 2. Basic design for an image plate detector with a cylinder geometry. A section though the cylinder is shown. The image plate is on the outside of the drum, which again is covered with the gadolinium neutron to γ-ray converter. For the recording of the accumulated light the read head slowly moves vertically while the central drum rotates at high speed. It is quite feasible to place the reading unit inside the drum, and such a model is presently being considered. Likewise, the drum could be evacuated or filled with He to reduce air-scattering.

while the cylinder rotates at high speed. In a final step the image plate surface is erased with light, and the next recording can begin.

5. A prototype detector

For the first prototype detector a horizontal geometry was chosen in order to simplify the bearing mechanics for the cylinder. The above discussed design parameters were used, and Fig. 3 shows a picture of the detector. The He–Ne laser is placed horizontally under the reading head, and the light is transmitted to the drum via mirrors placed to the right and on the moveable head. The released light is then recorded by a photomultiplier located on the reading head, and the rotating drum is scanned by a horizontal translation of the head. This movement is coupled electronically to the rotation of the drum.

For the tests the pixel size was selected to be 0.25 by 0.25 mm^2, which is also the final design goal. This gives a little over 6 Mpixels for the whole detector, and a reading time of about 5 min. The number of pixels can of course be reduced if the spot sizes are very large and this would lead to shorter reading times. For a zero-dimensional sample the full width at half height for 3 Å neutrons is 0.3 mm at the middle of the cylinder going to 0.8 mm at the edge following the expressions leading to (4). For the limit of very small crystals the target pixel size is therefore suitable. For large crystals there will be many pixel readings within the Bragg spot, and this can therefore either be used to reduce reading times or to employ the full data for profile analysis.

In the first test X-rays were used. A Fuji image plate model ST III with a dimension of 20.1 by 25.2 cm^2 was placed to record the diffraction pattern from a crystal of a mutant of seryl-tRNA synthethase. The recording took 10 min. with an oscillation angle of 0.05°, and afterwards the film was placed on the outside of the drum and read. Fig. 4 shows the diffraction pattern. The full width at half height of the low angle Bragg peaks was 0.5 mm, in agreement with values of 0.5 mm recorded with a MAR-RESEARCH detector under similar conditions. These values are in any case governed by the beam divergence and the crystal size.

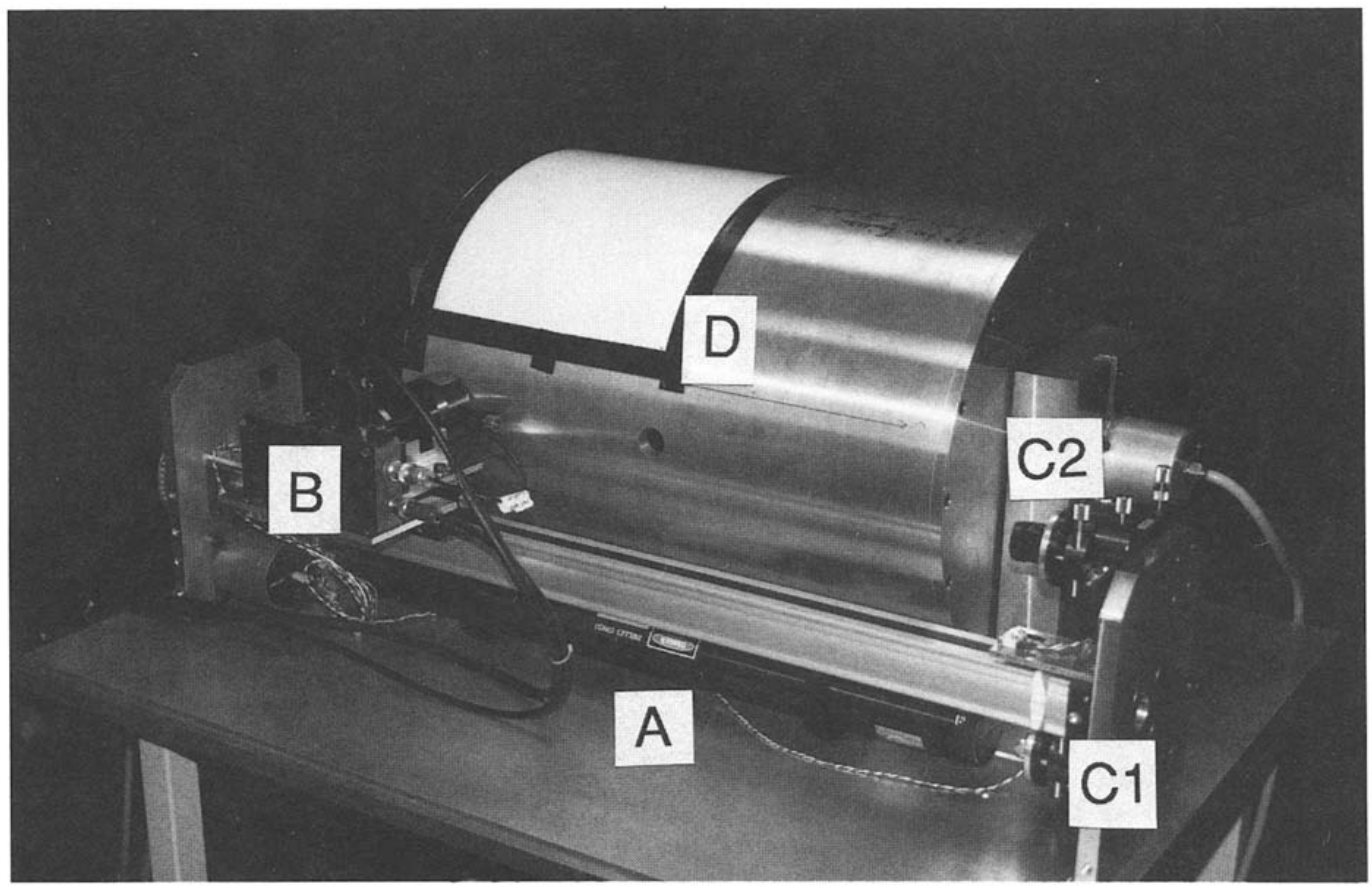

Fig. 3. Picture of the existing prototype. In this case the rotation axis is horizontal. The He–Ne laser which produces the red light for photo stimulation is located horizontally at the bottom (A), and the light is transferred to the read-head (B) via a double mirror placed to the right (C1, C2). The drive-shaft for the read head is located above the laser, while the motor is hidden below the table. At present only one image plate is placed on the drum and is seen at (D).

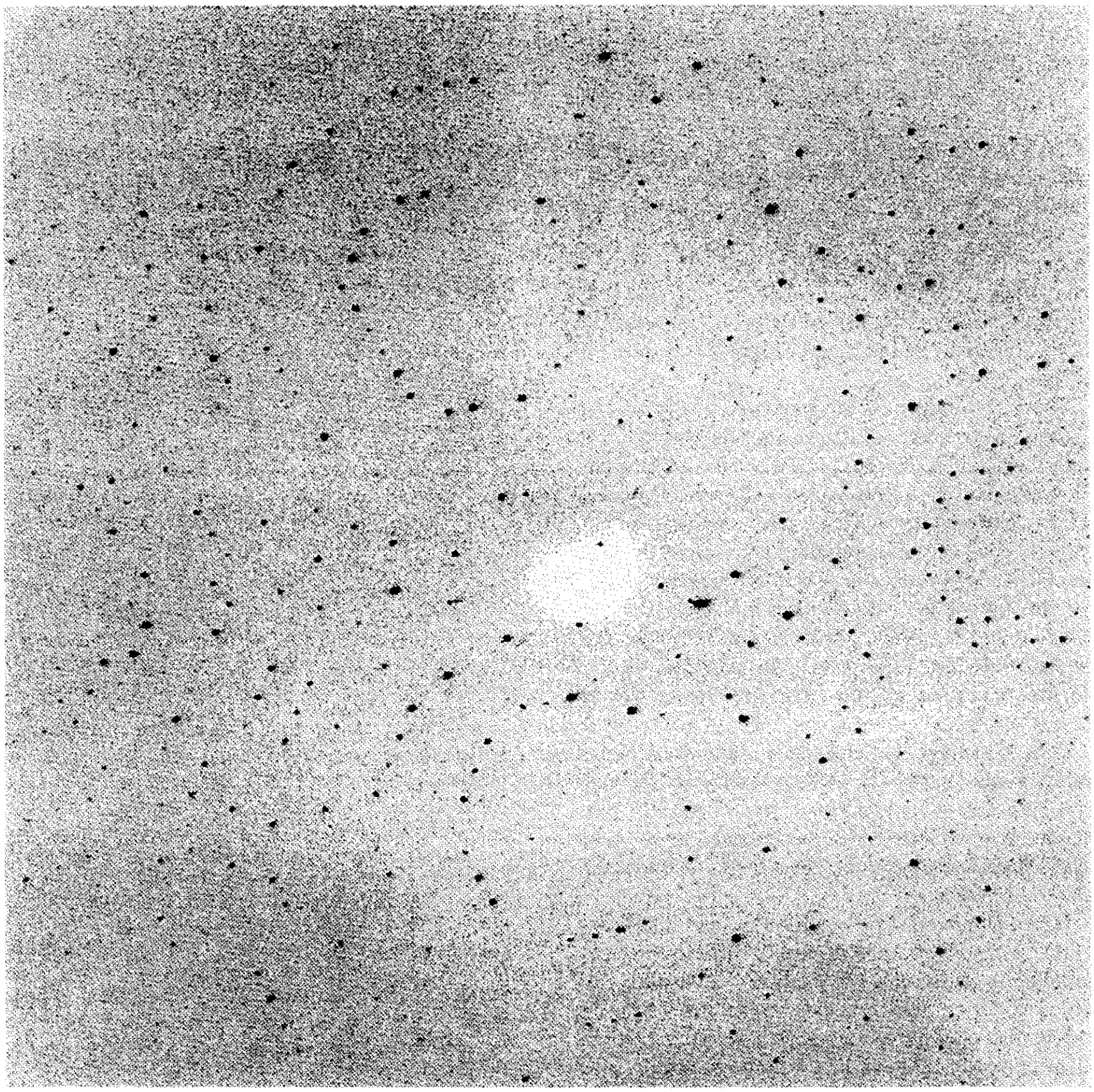

Fig. 4. The very first diffraction pattern recorded with the prototype. The space group of the protein crystal is $P2_1$ with cell axis $a = 80.15$ Å, $b = 170.27$ Å, $c = 91.12$ Å and $\beta = 124.88°$. The sample to film distance was 170 mm, and the picture which is the central part of the image plate holds 700 by 700 pixels.

Further tests and adjustments are now underway, but the first measurement clearly confirms the feasibility of the construction. In this X-ray test mode with off-line reading the detector resembles an earlier design by Amemiya et al. [22], and it is the plan also to use it as an off-line reader for large area image plates.

6. Concluding remarks

Many aspects of the detector still have to be studied. Some of these can only be done employing a neutron source, and work is now under way at the Institut Laue–Langevin to set up a simple beam-line for tests at the

reactor restart. The first tests will concern the sensitivity of the detector towards the inherent γ-background at a neutron source, and the detector efficiency.

Whenever a neutron is stopped (by an absorption process) γ-rays are produced. In many cases these are of MeV energy, and will not be visible to the image plate. However, any rescattering process will produce lower energy γ-radiation. The simplest way to reduce the γ-background is thus to place the detector as far from the reactor as possible and to ensure that the neutron beam is reduced to a small cross-section well before the instrument. The first test will therefore be carried out at the end of a cold neutron guide tube 150 m from the reactor core.

The detector efficiency is governed by the neutron conversion rate and the image plate sensitivity. The latter can attain high values [12], and the limiting factor is undoubtedly the neutron to γ-ray conversion. For long wavelength neutrons this can be as high as 70 to 80%. If however the conversion takes place in a foil outside the image plate, only half the quanta will go in the direction of the phosphor. It is therefore not likely with this type of system to obtain more than about 30% detection efficiency. There will also be a small reduction due to scattering in the image plate as the neutron passes through.

With the gadolinium embedded in the plate, higher values could possibly be obtained, but here the conversion process might take place so far inside the plate that the trapped state cannot be liberated by the laser irradiation. A final estimate must therefore await further experimentation.

It is of paramount importance in neutron diffraction studies to use very large position sensitive detectors. Combining the earlier observations [13,14,17] that neutrons can be detected using image plates with the present first tests of the drum detector, which confirms its mechanical stability, does seem to indicate, that a large cylindrical neutron detector based on image plate technology can be successful.

Acknowledgements

The prototype image plate is being built with financial support from Professor G. Büldt of the Freie University, Berlin, and we are very thankful to him and to Dr. K. Bartels from the same group for many useful discussions. We are also very grateful towards Dr. H. v. Seggern, Siemens, Erlangen, who supplied the gadolinium containing image plate, we thank Dr. Carmen Berthet, EMBL, Grenoble, for use of her protein crystal in recording the spectra in Fig. 4, and Dr. H. Boerner for explanation of the gadolinium neutron capture process.

References

[1] B.P. Schoenborn, Nature 224 (1969) 143; J.P. Bouquiere, J.L. Finney and M.S. Lehmann, J. Chem. Soc. Faraday Trans. 89 (1993) 2701; J.P. Bouquiere, J.L. Finney, M.S. Lehmann, P.F. Lindley and H.J.F. Savage, Acta Cryst. B 49 (1993) 79; X. Cheng and B.P. Schoenborn, Acta Cryst. B 46 (1990) 195; A.A. Kossiakoff, M.D. Sinchak, J. Sphungin and L.G. Presta, Proteins Struct. Funct. Gen. 12 (1992) 223; A.A. Kossiakoff, M. Ultsch, S. White and C. Eigenbrot Biochemistry 30 (1991) 1215; A. Wlodawer, J. Walter, R. Huber and L. Sjölin, J. Mol. Biol. 180 (1984) 301.

[2] A. Lewit, P.A. Timmins, G.A. Bentley, B. Jacrot and J. Witz, Abst. 4th Eur. Cryst. Meeting (Oxford, 1977) pp. 1–138; M. Eisenstein, R. Sharon, Z. Berkovitz-Yellin, H.S. Gewitz, S. Weinstein, E. Pebay-Peyroula, M. Roth and A. Yonath, Biochimie 73 (1991) 879; M. Roth, A. Lewit-Bentley, H. Michel, J. Deisenhofer, R. Huber and D. Oesterhelt, Nature 340 (1989) 659; P.A. Timmins, B. Poliks, B. and L. Banaszak, Science 257 (1992) 652.

[3] B.P. Schoenborn, SPIE 1737 (1992) 235.

[4] M. Thomas, R.F.D. Stansfield, M. Berneron, A. Filhol, G. Greenwood, J. Jacobé, B. Feltin and S.A. Mason, in: position-sensitive detection of thermal neutrons, eds. P. Convert and J.B. Forsyth (Academic Press, New York, 1983) p. 344.

[5] M.G. Strauss, R. Brenner, F.J. Lynch and C.B. Morgan, IEEE Trans. Nucl. Sci. NS-28 (1981) 800.

[6] A.J. Schultz, K. Srinivasan, R.G. Teller, J.M. Williams and C.M. Lukehart, JACS 106 (1984) 999.

[7] M. Roth, A. Lewit-Bentley and G.A. Bentley, in: position-sensitive detection of thermal neutrons, eds. P. Convert and J.B. Forsyth (Academic Press, New York, 1983) p. 339.

[8] C. Wilkinson and M.S. Lehmann, Nucl. Instr. Meth. A 310 (1991) 415.

[9] P. Thomas, J. Appl. Cryst. 5 (1972) 83.

[10] J. Baruchel, in: Neutron and synchrotron radiation for condensed matter studies, eds. J. Baruchel, J.-L. Hodeau, M.S. Lehmann, J.-R. Regnard and C. Schlenker (Springer/Les Editions de Physique, Berlin, 1993) p. 399.

[11] J.C. Marmeggi, in: Methods of structural analysis of modulated structures and quasicrystals, eds. J.M. Pérez-Mato, F.J. Zuniga and G. Madriaga (World Scientific, Singapore, 1992) p. 448.

[12] Y. Amemiya, T. Matsushita, A. Nakagawa, Y. Satow, J. Miyahara and J. Chikawa, Nucl. Instr. Meth. A 266 (1988) 645.

[13] C. Rausch, T. Bücherl, R. Gähler, H. von Seggern and A. Winnacker, SPIE 1737 (19932) 255.
[14] C. Wilkinson, A. Gabriel, M.S. Lehmann, T. Zemb and F. Né, SPIE 1737 (1992) 324.
[15] H. Rauch, F. Grass and B. Feigl, Nucl. Instr. Meth. 46 (1967) 153.
[16] A. Backlin, G. Hedin, B. Fogelberg, M. Saraceno, R.C. Greenwood, C.W. Reich, H.R. Koch, H.A. Baader, H.D. Breitig, O.W.B. Schult, K. Schreckenbach, T. von Egidy and W. Mampe, Nucl. Phys. A 380 (1982) 189.
[17] H. von Seggern, K. Schwarzmichel, T. Bücherl and C. Rausch, in: Proceedings of the EPDIC-3 (1994), in press.
[18] A. Harms and D.R. Wyman, Matematics and physics of neutron radiography (Reidel, Dordrecht, 1986).
[19] J.A.K. Howard, O. Johnson, A.J. Schultz and A.M. Stringer, J. Appl. Cryst. 20 (1987) 120.
[20] R.P. May, K. Ibel and J. Haas, J. Appl. Cryst. 15 (1982) 15.
[21] J.D. Bernal, Proc. Roy. Soc. A 153 (1926) 157.
[22] Y. Amemiya, S. Kishomoto, T. Matsushita, Y. Satow and M. Ando, Rev. Sci. Instrum. 60 (1989) 1552.